Proceedings, Bicycle and Motorcycle Dynamics 2010
Symposium on the Dynamics and Control of Single Track Vehicles,
20 - 22 October 2010, Delft, The Netherlands

Steering Characteristics of Motorcycles

S. Fujii*, S. Shiozawa*, A. Shinagawa*, T. Kishi*

*YAMAHA MOTOR CO., LTD.
2500 Shingai, Iwata, Shizuoka, 438-8501, Japan
E-mail: fujiis@yamaha-motor.co.jp

ABSTRACT
In this study, the results of a steady-state cornering test using a sport-touring motorcycle and the analysis of those test results are presented. This test was conducted as one activity in our efforts to realize a quantitative development method for motorcycles. The measurement data from this test include measurement results for tire force, tire moment, and tire slip angle that have not been practically addressed in the research of motorcycles, in addition to normal measurement results for velocity, steering angle, steering torque, roll angle, and the like.
Up to now research on motorcycle dynamics characteristics has indicated that "there is a strong relationship between the motorcycle dynamics characteristics and the tire slip angle". However, since it is difficult to take highly precise measurements of the motorcycle's tire slip angle during actual riding, especially when the motorcycle is tilted during cornering, such measurements have been avoided.[1] Nevertheless, in this research we attempted to measure the tire slip angle and also attempted to investigate in detail the dynamics characteristics and tire characteristics during riding. Up to this point there has not been an adequate investigation conducted under a variety of riding conditions, but it is the aim of this research to show that it is possible to measure the tire slip angle with good accuracy. It is our opinion that this will open a new path to a more detailed investigation of the motorcycle's dynamics characteristics.
In addition, we conducted measurements using not only the normal rider's lean angle (lean-with posture), but also measurements in the case where the rider's lean angle was intentionally changed, in order to investigate the effects that a change in the rider's posture has on the variation in the measurement results of the motorcycle's dynamics. Furthermore, we then compared these measurement results to the results obtained from simulations. Additionally, steering index values were calculated from the measurement results. These calculated index values include the stability factors, slip angle factors, and steering torque factors.

Keywords: motorcycle, steering characteristics, steady-state cornering, tire slip angle, lean angle

1 INTRODUCTION
As the motorcycle market continues to mature and the need for improved safety and running through performance increases, more and more manufacturers are installing electronic control devices used in four-wheeled vehicles to control vehicle dynamics. While the installation of electronic control devices makes it possible to fine-tune the performance of motorcycles, the resultant increase in development cost for selecting the optimum control parameters has become a serious issue. Therefore, in order to efficiently optimize the control parameters, a "quantitative development method" is needed that can predict the maneuverability for each control parameter and rationally select the optimum control parameters from the viewpoint of maneuverability. In order to make such quantitative development possible it will be necessary to (1) construct measurement technologies that can quantitatively grasp vehicle dynamics characteristics in greater detail, (2) construct simulation technology that can predict the ride of the vehicle based on its characteristic values, and (3) decide on the quantitative evaluation indexes that can be used for determining whether the predicted or measured ride is good or not.

The research conducted up to now, such as that in Reference [1], has indicated that "there is a strong relationship between the motorcycle dynamics characteristics and the tire slip angle". However, since it is difficult to take highly precise measurements of the motorcycle's tire slip angle during actual riding, especially when the motorcycle is tilted during cornering, such measurements have been avoided. Therefore, it was attempted to estimate the tire slip angle by first measuring the tire characteristics in advance via a bench test and then assuming that these characteristics would not change during actual riding. Then the tire lateral force (Fy) was divided into the component that originates from the camber angle, and the one that originates from the tire slip angle. This enabled the estimation of a general value for the tire slip angle, but since it was assumed that the tire characteristics from the bench test are the same as the tire characteristics during actual riding it was not possible to investigate changes to the tire characteristics produced by the heat generated during riding or other factors. Therefore, in this research we set out to measure the tire slip angle as an activity to realize a quantitative development method and also as a measurement technology to quantitatively grasp vehicle dynamics characteristics in greater detail. This research has not yet led to an investigation of the tire slip angle under a variety of riding conditions, but it is the aim of this research to show that it is possible to measure the tire slip angle with good accuracy. Consequently, it is our opinion that this will open a new path to a more detailed investigation of the motorcycle's dynamics characteristics.

A slight shift in the way that a motorcycle rider moves his/her body will significantly change the motorcycle's dynamics characteristics and, in addition, when complicated operations of the steering, throttle, brakes, and the like are performed, this makes it difficult to obtain measurements with a high level of repeatability. Therefore, in order to try out a new measurement method, such as measuring the tire slip angle, it is our opinion that first it is appropriate to conduct the evaluation using the steady-state cornering test, which is thought to have a high level of repeatability. The results reported in this study are therefore limited to those from the steady-state cornering test. Next, we investigated the effect that a change in the rider's lean angle has on the ride since the lean angle also has a large effect on the variation in the measurement results. Consequently, ride data was obtained in the case where the rider's lean angle was intentionally changed in order to show the effect that it caused.

Many simulation technologies have been studied. However, a comparative verification of the simulation results and the actual ride data have rarely been published. Therefore, in this research the measurement data for the tire slip angle, tire force, and other results were compared to the results obtained from simulations.

Finally we will discuss the activities related to the evaluation indexes. Kageyama et al. [2] proposed a steering index for the steady-state cornering characteristics of motorcycles and showed its theoretical background, as well as its differences from the steering index for four-wheeled vehicles. It is our opinion that it is necessary to determine the numerical values that represent the vehicle characteristics, such as the stability factors for four-wheeled vehicles, and to also accumulate the characteristic values of many vehicles in order to realize the quantitative development method for motorcycles. However, activities to validate the index against actual ride data have been insufficient. In this research, we calculated steering indexes from the actual measurement result data for the stability factors, the slip angle factors, and steering torque factors.

2 MEASUREMENT METHOD

For our study, we used a large sport-touring motorcycle with 1,300-cc displacement. The riding method used steady-state cornering in both the clockwise and counterclockwise directions at various velocities on courses with 20-, 30-, and 50-m radiuses. We measured the steering angle, steering torque, vehicle velocitiy, roll angle, tire force, tire moment, and tire slip angle, and used an ISO coordinate system to display the measurement results as shown in Fig. 1. Here, the steering angle is an angle of motion of the steering assembly about the steer axis which is zero when the front wheel plane is parallel to the motorcycle longitudinal plane.

For measuring the tire slip angle, we used an inertia & GPS posture sensor (hereafter referred to as the “inertia GPS sensor”) shown in Fig.2 and an optical 2-axis speed sensor (hereafter referred to as the “optical slip sensor”) shown in Fig.3 simultaneously, and compared their measurement results.

The inertia GPS sensor used acceleration and angular velocity data measured by an inertia sensor and positional data measured by a GPS, and employed a process such as Kalman filtering to determine the longitudinal and lateral velocities in the rear seat position where the sensors were installed. Then, based on the 2-axial speed at the sensor position, and using a conversion equation that uses data such as the yaw rate, roll rate, steering angle and relative position of tire's contact point to the sensor position, the longitudinal and lateral velocities corresponding to the tire direction at the contact points of the front and rear tires were determined and converted into tire slip angles.[7]

Meanwhile, the optical slip sensors installed ahead of the front wheel and behind rear wheel determined the forward and lateral velocities directly below the sensors, corrected them for the yaw rate and the difference between the front and rear positions, and determined the tire slip angles at the tire contact points as shown in Fig.4. [8]

Additionally, we installed wheel load sensors for both tires, as shown in Fig.5, in a vehicle identical to the one for which the tire slip angles were measured, to measure the tire force and tire moment. The wheel load sensor converts strain gauge signals on each spokes into the tire forces and moments respectively.

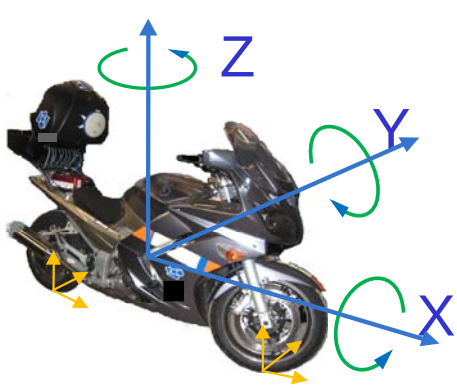

Figure 1. Coordinate system

Position Accuracy	1.8 mCEP
Velocity Accuracy	0.1 km/h RMS
Heading	0.1 ° 1σ
Roll / Pitch	0.05 ° 1σ
Slip Angle	0.2 ° RMS

※ quote from manual [7]

Figure 2. Inertia GPS sensor

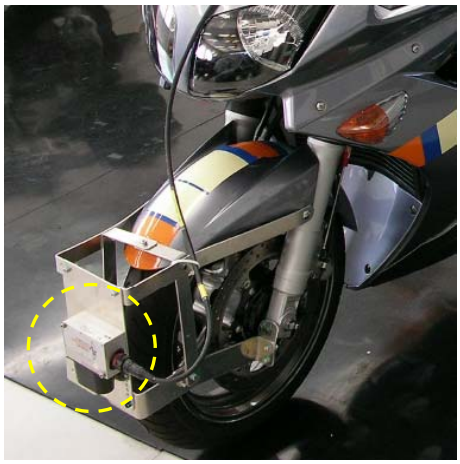

Distance Resolution	2.47 mm
Distance Measurement Deviation	< ± 0.2 %
Angle Resolution	< ± 0.1 °

※ quote from manual [8]

Figure 3. Optical slip sensor

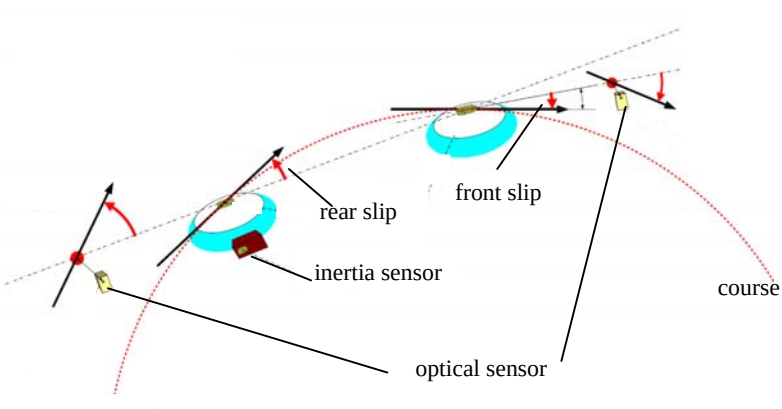

Figure 4. Slip measurement sensor arrangement

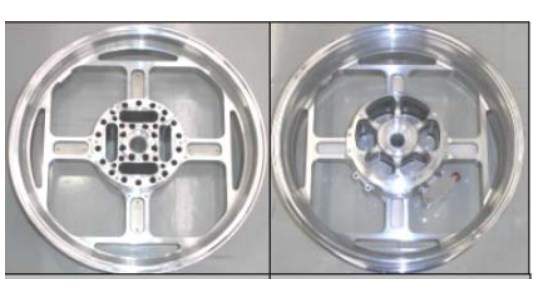

Figure 5. Wheel load sensor

3 Simulation Model

We used MATLAB/Simlink/SimMechanics to create a body model for simulation. As shown in Fig. 6, this model was created to have ten rigid bodies(main frame, rider, engine, tank, front fork, front arm, front wheel, arm relay, rear arm, and rear wheel), four rotating joints (steering, rear arm pivot, front wheel, and rear wheel), one expansion joint (front suspension), and two spring dampers (front suspension and rear suspension). We gave the model a total of 11 degrees of freedom, that is, six for the reference point of the main frame (forward-backward, left-right, up-down, roll angle, pitch angle, and yaw angle), plus the rotation of the front and rear wheels, the expansion of the front suspension, the rotational angle of the rear arm, and the rotational angle of the steering. For the external forces, gravity, air resistance, lift, and tire load were used in the model. The input data were individual rigid bodies' coordinate values of the centers of gravity and linking points, weight, and moments of inertia as well as the property values such as spring and damper, and the tire constants.[3,4]

For the tire model, MF-Tyre was used. This model uses the tire's state relative to the road surface (height, camber angle, tire slip angle, and slip ratio) as its input, and utilizes the parameters obtained for each tire to output the longitudinal and lateral forces, tire vertical load, self-aligning torque, rolling resistance moment, and overturning moment at the tire contact point. For the model's parameters, the measurement values were used to fit.

The running simulation is executed with a rider control model which control the vehicle body model such that a reference roll angle and a reference velocity are achieved. In the rider control model, the drive torque τ d and steering torque τ s are respectively calculated using the following equations:

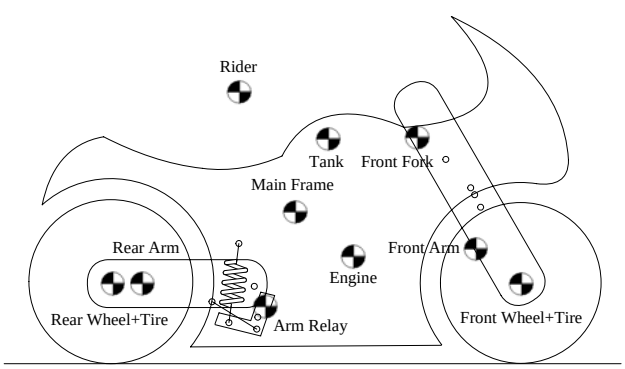

Figure 6. Body model of Simulation

$$\tau_d = -K_{p1}\left(v - v_{ref}\right) \tag{1}$$

$$\tau_s = -K_{p2}\left(\varphi - \varphi_{ref}\right) - K_{d2}\dot{\varphi} - K_{d3}\dot{\alpha} \tag{2}$$

v: forward velocity (m/s)

ϕ : roll angle (deg)

α : steering angle (deg)

v ref: reference value of forward velocity (m/s)

ϕ ref: reference value of roll angle (deg)

τ d: driving torque(Nm)

τ s: steering torque(Nm)

Kp1: velocity deviation proportional gain for drive torque

Kp2: roll angle deviation proportional gain for steering torque

Kd2: roll rate gain for steering torque

Kd3: steering angle rate gain for steering torque

P/D control is used to match the velocity and the roll angle to the reference velocity and the reference roll angle, to which the effect of the steering damper is added. The term of the steering damper is normally provided in the vehicle body model. However, we added it to Equation 2 because the friction that occurs in the steering system is normally small and is actually a force added by the rider, and because the steering damper value will change depending on the riding conditions. Note that in our simulation, the reference roll angle was adjusted in order to achieve a ride with the desired turning radius, and each P/D gains in the ride model for achieving a stable ride were determined in advance using a genetic algorithm for each reference velocity and reference roll angle. During the simulation, the optimum value was selected according to the riding condition.

4 MEASUREMENT AND SIMULATION RESULTS

Fig. 7 shows the simulation results corresponding to the data from a clockwise, steady-state cornering test conducted at a turning radius of 50 m and at a velocity of 65 km/h. In the riding test, as can be seen from the locus data and velocity data shown in the figure, the vehicle first accelerated over a 50-m linear section from a fully-stopped state, then entered a circular track which it circled once, and finally returned to a straight extension of the linear section, where it decelerated. The simulation, on the other hand, was executed with the initial velocity set nearly constant and equal to the reference velocity and using the reference course used in the riding test as the reference course.

The data shows that the velocity, roll angle, and steering angle were nearly constant in both the actual measurements and the simulation during the period between the 12th and 22nd seconds, and therefore this period was assumed to correspond to the steady-state cornering section. The measurement results essentially matched the simulation results. However, whereas the steering angle, steering torque, and tire slip angle were constant in the aforementioned section in the simulation, only the steering angle was nearly constant in the measurement values. The steering torque and tire slip angle continued to change in one direction as if drifting during cornering. This phenomenon was especially noticeable when the roll angle and velocity were large, and is presumed to be intimately related to rises in the tire temperature.

In this example, the steering torque remained positive. Positive values in this case indicate a counterclockwise direction. In other words, they indicate that a torque opposite from the corning direction was applied during clockwise cornering, and counter steering torque was applied in order to prevent the steering bar from turning too far in the cornering direction. In the example shown here, the steering torque value then dropped when cornering was continued.

The tire slip angle is defined as being positive in the direction toward the left side of the driving direction. The tire slip angle of the front wheel was negative according to both the inertia GPS sensor and the optical slip sensor in this example, indicating the direction toward the cornering center. On the other hand, the tire slip angle of the rear wheel was positive, indicating the direction away from the cornering center.

In the example shown, as cornering continues, the tire slip angle of both the front and rear wheels gradually changed away from the cornering center (in the positive direction in this example). The data from both the inertia GPS sensor and the optical slip sensor are passed through a 1-Hz low-pass filter process, but the result from the inertia GPS sensor was smoother. Furthermore, the measurement values from both sensors tended to be unstable at low velocities in some cases.

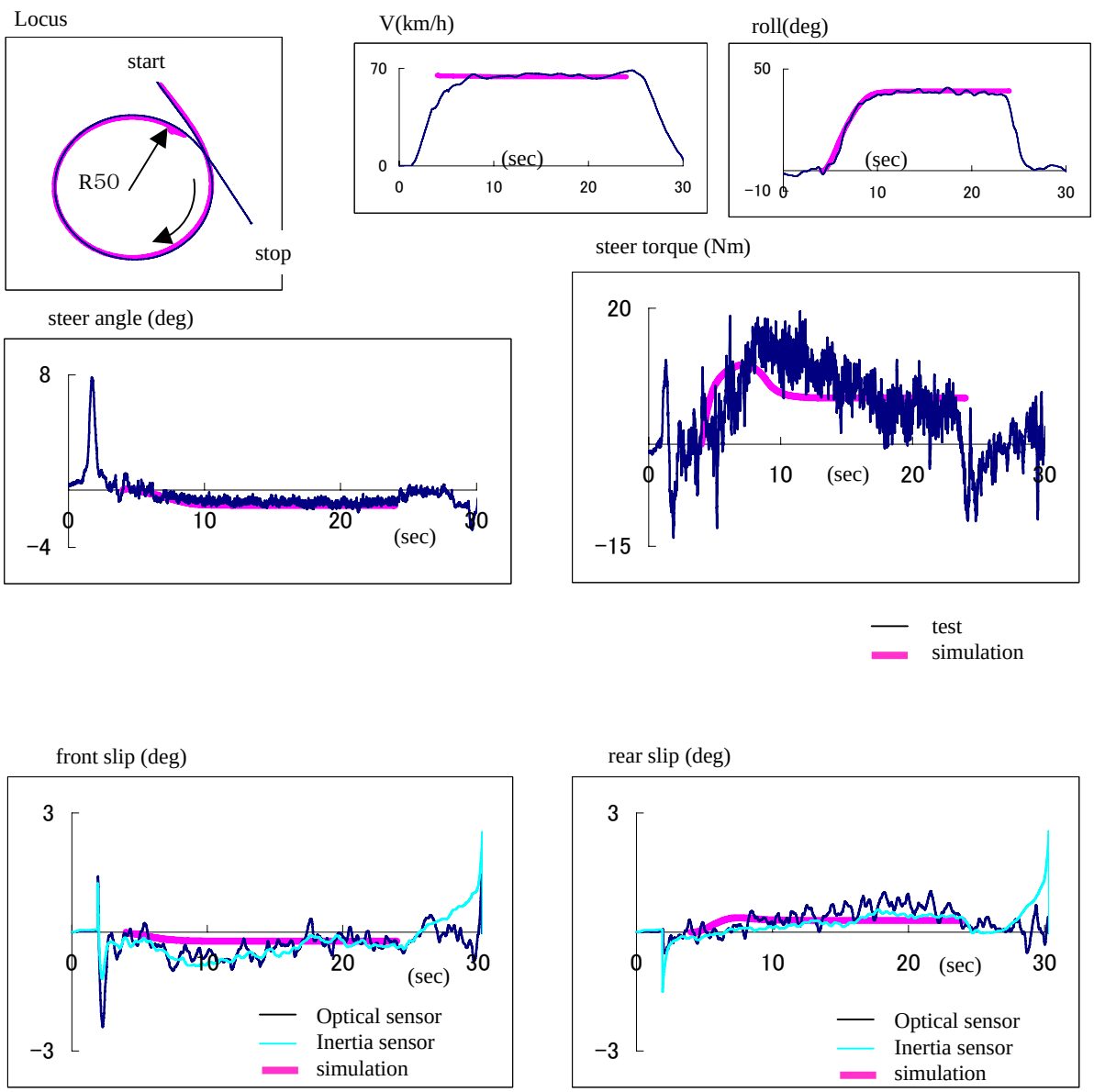

Figure 7. Time series data

In the following section, the average values of the steady-state cornering data obtained under different conditions are compared. In this case, a single average value is obtained by averaging the values for a 5-second period in which the velocity, roll angle, and steering angle become nearly constant.

Fig. 8 is a graph in which the horizontal axis is assigned to the vehicle body roll angle, and compares the average values of the tire slip angle at the front and rear wheel contact points during steady-state cornering with a 50-m radius, based on the results from the inertia GPS sensor, the optical slip sensor, and the simulation. Although the variation in the measurement results is large, the three results essentially match each other. The tire slip angle described in the following section is the value measured by the optical slip sensor.

Figs. 9 and 10 show the averaged measurement results for the steering angle, hold-steering torque, front and rear tire slip angles, front and rear tire forces, and front and rear tire moments during a steady-state ride in steady-state cornering with a 50-, 30-, and 20-m radius, along with the simulation results. The steering angle varied little and closely matched the simulation result. In contrast, the hold-steering torque varied widely. However, if the roll angle is kept the same, the steering torque also matches the simulation result in that it increases as the turning radius decreases.

The front tire slip angle varied greatly, showing no clear differences among the different turning radii. The manner in which the front tire slip angle changed in response to the roll angle was similar to that in the simulation result.

The rear tire slip angle also showed few differences among the different turning radii, but did show the same trend as in the simulation results.

Fy (CPI) for both the front and rear wheels is a value that is proportional to the roll angle regardless of the circle radius, and matched the simulation results well.

The moment Mx (STI) of the rear tire did not show any differences among the different circle radii, while Mx of the front tire did show such differences, and showed the same trend as in the simulation results. It is presumed that this difference is linked to the difference in the hold-steering torque among the different circle radii. The moment Mz (STI) did not show distinct differences among the different circle radii for the both tires and essentially matched the simulation results.

(Note) (STI indicates the tire force in a coordinate system that uses the center of the tire as the origin and in which the coordinate axes match the tire movements. CPI indicates the tire force in a coordinate system that uses the contact point between the tire and the road surface as the origin and in which the coordinate axes follow the road surface. See Fig. 11. For details, see [5].)

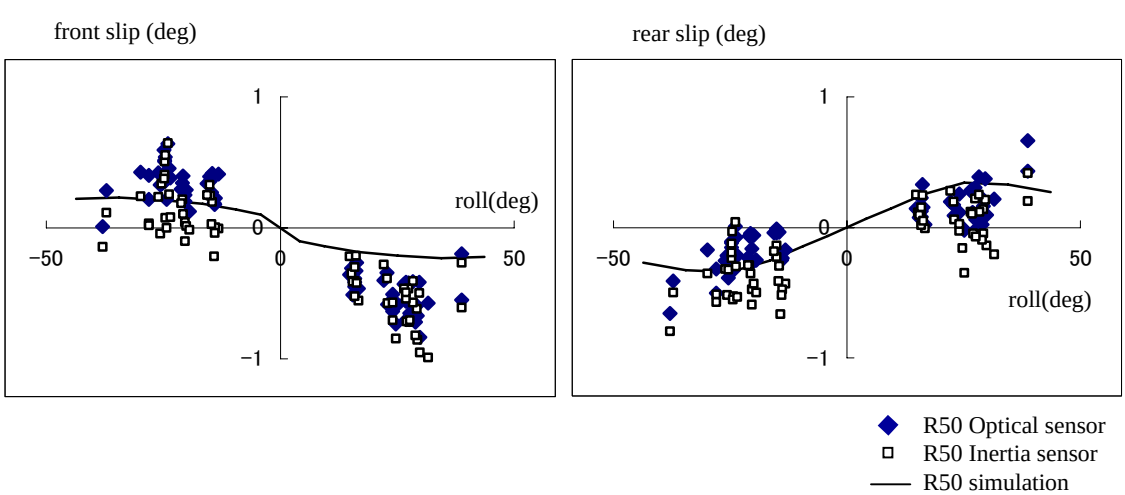

Figure 8. Slip angle data comparison between optical and inertia sensor

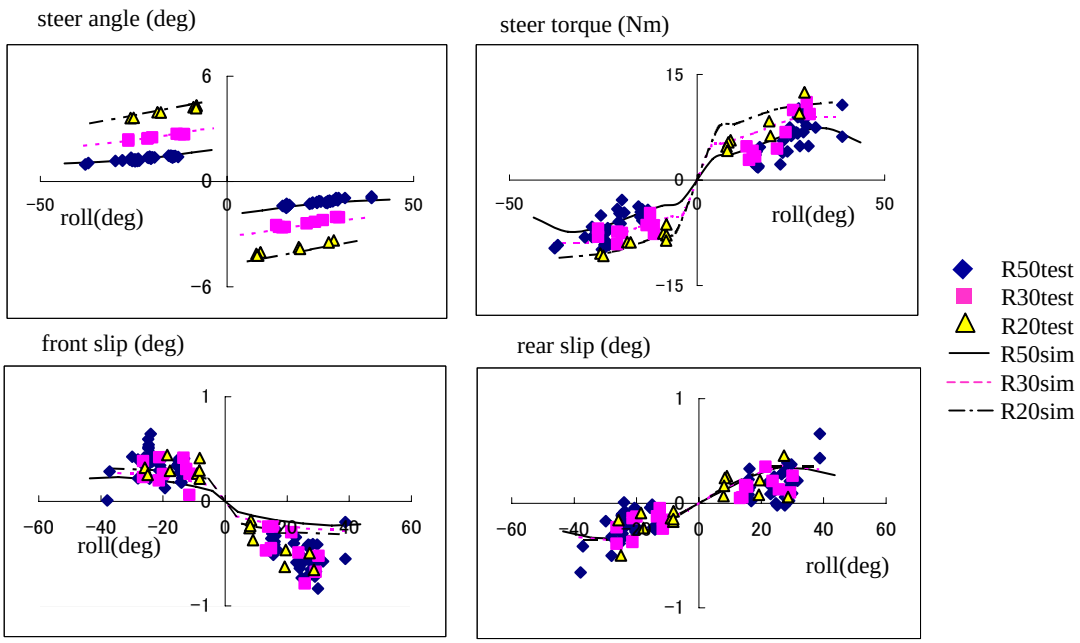

Figure 9. Average data changing circle radius

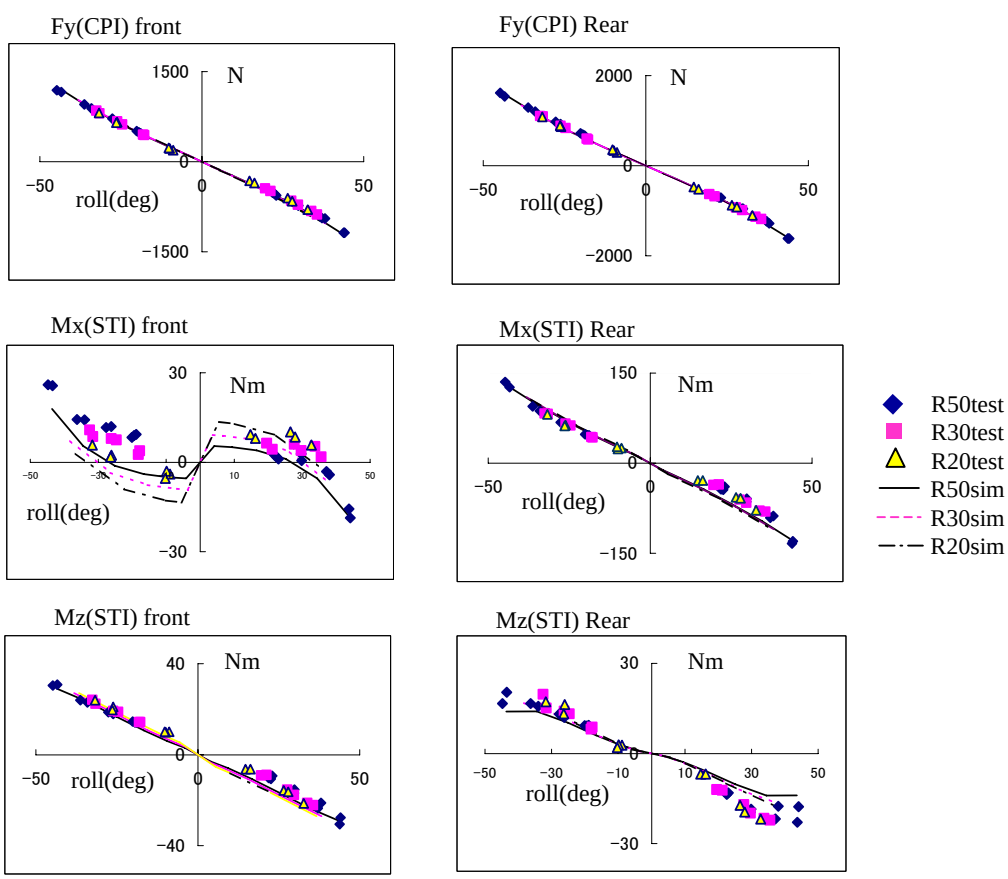

Figure 10. Wheel load data changing circle radius

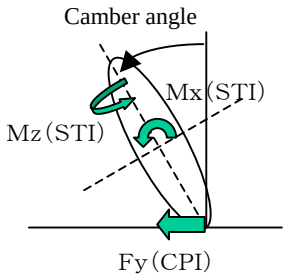

Figure 11. Tire force and moment (front view)

5 IMPACT OF RIDER LEAN ANGLES ON MEASUREMENT RESULTS

While last chapter shows only the measurement data obtained when the rider was instructed to maintain a lean-with posture, this chapter compares the differences in data with the rider assuming the lean-in, lean-with, and lean-out postures as shown in Fig.12. Note that, for purposes of evaluation, the graphs in this chapter also show the simulation results obtained by shifting the rider's weight by 10 cm to the right or left while the motorcycle was kept upright, along with the aforementioned three types of measurement data.

As shown in Fig. 13, when the rider assumed the lean-in posture, the absolute value of the steering angle increased, and either counter steering torque decreased or anti-counter steering torque occurred in terms of hold-steering torque in some cases. Additionally, the absolute value of the front tire slip angle decreased and tended to move away from the cornering center. On the other hand, the rear tire slip angle increased in the direction moving away from the cornering center. These trends were the same in the simulation, and the data obtained when the weight was shifted to the right corresponded to the lean-in result during rightward cornering (with a positive roll angle) and to the lean-out result during leftward cornering (with a negative roll angle). In both cases, the data showed the same trend.

Furthermore, as shown in Fig. 14, Fy (CPI) shows little changes. However, a closer look reveals that Fy (CPI) for both the front and rear wheels increased, albeit slightly, given the same roll angle, as the tire slip angle changed in the lean-in case. Mx (STI) for both the front and rear wheels also increased in the direction restoring the roll angle. Mz (STI) did not show clear differences, but the absolute values for both the front and rear wheels decreased.

It is presumed that these changes were caused by the following factors: Because the lean-in posture generated a moment in the direction of increasing the roll angle, a greater restorative moment to counteract it became necessary, as a result increasing the tire slip angle for both the front and rear wheels in the direction away from the cornering center, which in turn increased the cornering force. Note that during cornering with the same circle radius, the lean-in posture resulted in a smaller roll angle than the lean-with posture.

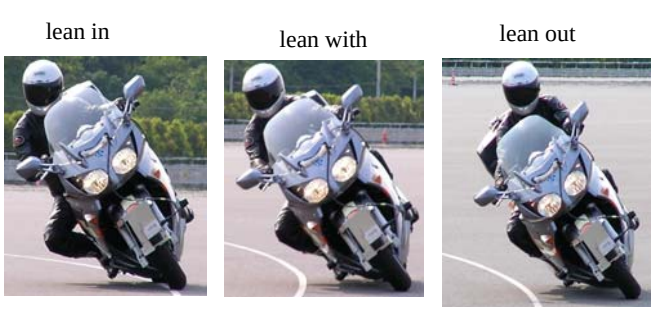

Figure 12. Rider's posture difference

The reduction in the hold-steering torque during the lean-in posture is presumed to be caused primarily by changes in Mx (STI) for the front-wheel, but changes in Mz (STI) also contributed. It is also possible to consider that the reduction in the steering torque was caused by an increase in the cornering force, which was caused by changes in the front tire slip angle.

When the lean-in posture causes the hold-steering torque to become 0, cornering can be maintained even with the rider's hands off the handlebar. If the rider does not lean in, he/she must hold down the handlebar to prevent it from turning too far toward the cornering side in order to complete the cornering maneuver. However, if this trend is strong, so-called "reverse steering", in which the handlebar is turned away from the turning direction, becomes necessary. Therefore, with a vehicle that requires a large hold-steering torque, the rider must lean far or employ reverse steering in order to begin turning; therefore, such a vehicle tend to be rated as having a strong tendency to continue going straight or as being difficult to turn. In contrast, with a vehicle that requires a small hold-steering torque, the rider can begin turning by simply shifting weight and without being conscious of moving the handlebar; therefore, such a vehicle tends to be rated as being easy to turn.

When the rider maintained the lean-out posture, the absolute value of the steering angle decreased while the steering torque increased. The front tire slip angle increased in the direction toward the cornering center. The rear tire slip angle decreased in the direction away from the cornering center. When the rider assumed the lean-out posture, the lateral force slightly decreased in the tire force, the opposite of when the rider assumed the lean-in posture, and Mx (STI) changed in the direction opposite from the direction for restoring the roll while Mz (STI) increased slightly toward the side where the roll angle occurs.

These results showed the same trends as in the simulation results.

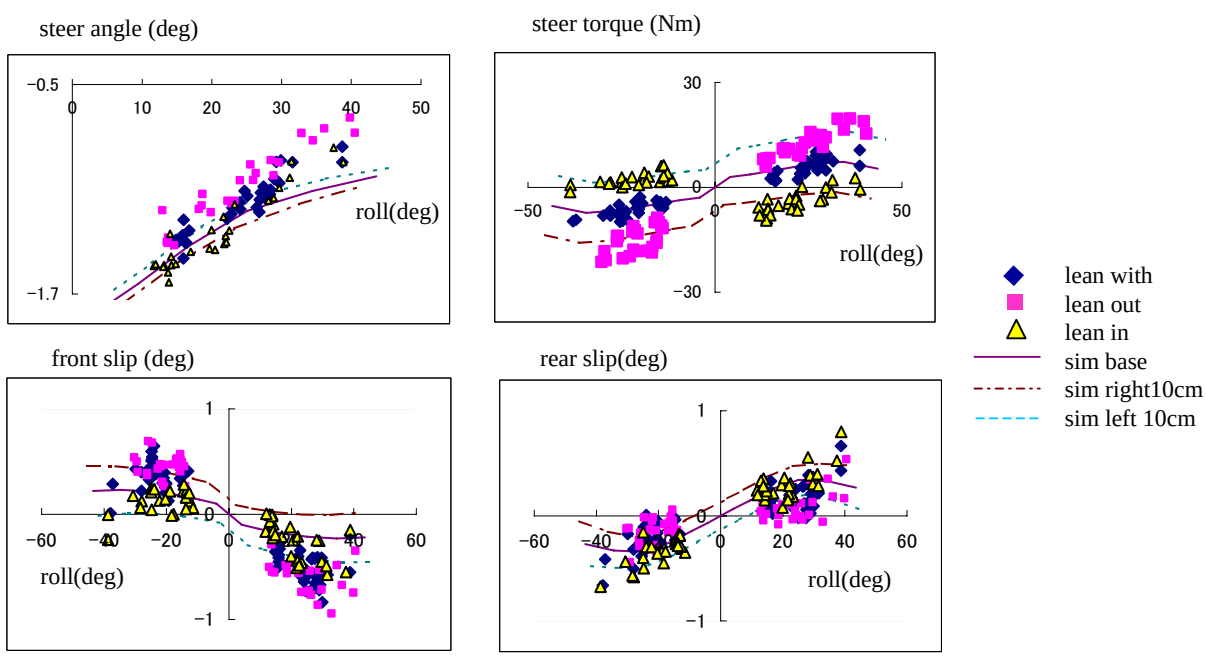

Figure 13. Averaged data changing rider lean (R50)

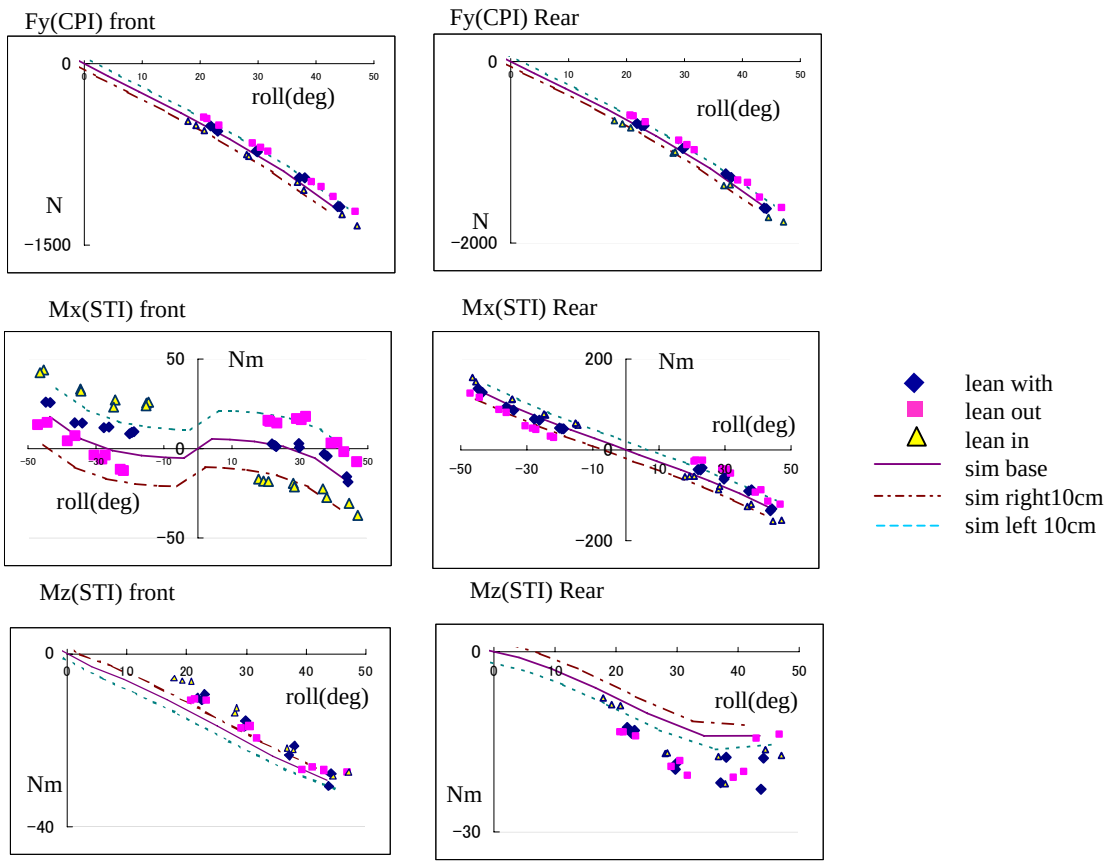

Figure 14. Wheel load data changing rider lean (R50)

6 STEERING INDICES

In this chapter, we will use the measurement results described so far and calculate the characteristic values related to the maneuverability during steady-state cornering proposed by Kageyama et al. [2]

Following the examples in References [2], Figs. 15 and 16 show the relationship between the square of the velocity and the absolute values of the steering angle, the tire slip angle at the center of gravity and hold-steering torque. We also used the following equation described in Reference [2] and the geometric steering angle values to determine the stability factors.

$$\frac{\delta}{\delta_0} = \delta \times \frac{R}{l} \times \frac{\pi}{180} = 1 + K_\delta \times V^2 \tag{3}$$

δ : Steering angle (deg)

$\delta_0 (= \frac{l \times 180}{R \times \pi})$: Geometric steering angle (deg)

R : Turning radius(m)

l : Wheelbase(m)

K_δ : Stability factor (s^2 / m^2)

V : Vehicle's forward velocity(m / s)

We also used the following equations to determine the slip angle factor and steering torque factor.

$$\frac{\beta}{\beta_0} = 1 + K_\beta \times V^2 \tag{4}$$

β : Slip angle at the center of gravity of motorcycles(deg)

$\beta_0 (= \frac{l_1}{R})$: Geometric slip angle (deg)

l_1 : distance between rear tire center and center of gravity in the longitudinal direction(m)

K_δ : Slip angle factor (s^2 / m^2)

$$\tau = K_\tau \times V^2 \tag{5}$$

τ : Steering torque(Nm)

K_τ : Steering torque factor (Ns^2 / m)

Table 1 shows the stability factors obtained. The results show negative values, which indicate over-steering. The relationship between the square of the velocity and the absolute value of the steering angle is linear at all turning radii, and as shown in Fig. 16, this slope did not change much, even when the lean angle changed. Therefore, this factor appears promising as an index. The lines in the graph for steering angle in Fig. 15 and Fig. 16 were drawn from the intercepts which meant the geometric steering angles and followed the data by the least squares method.

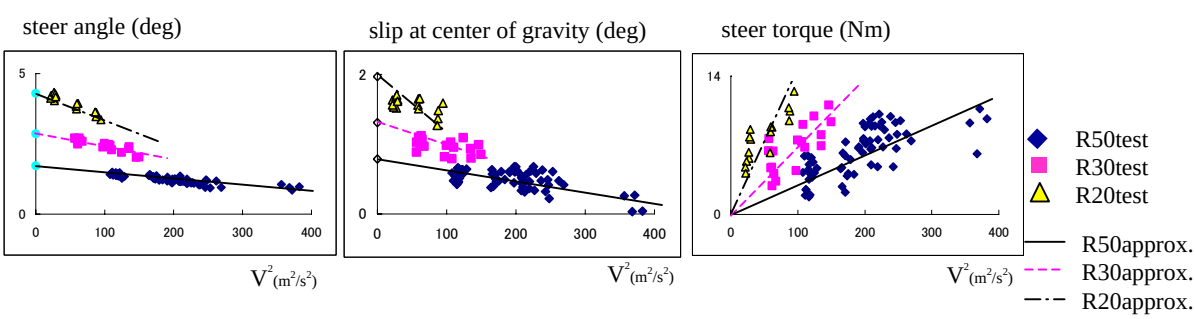

Figure 15. Averaged data changing circle radius

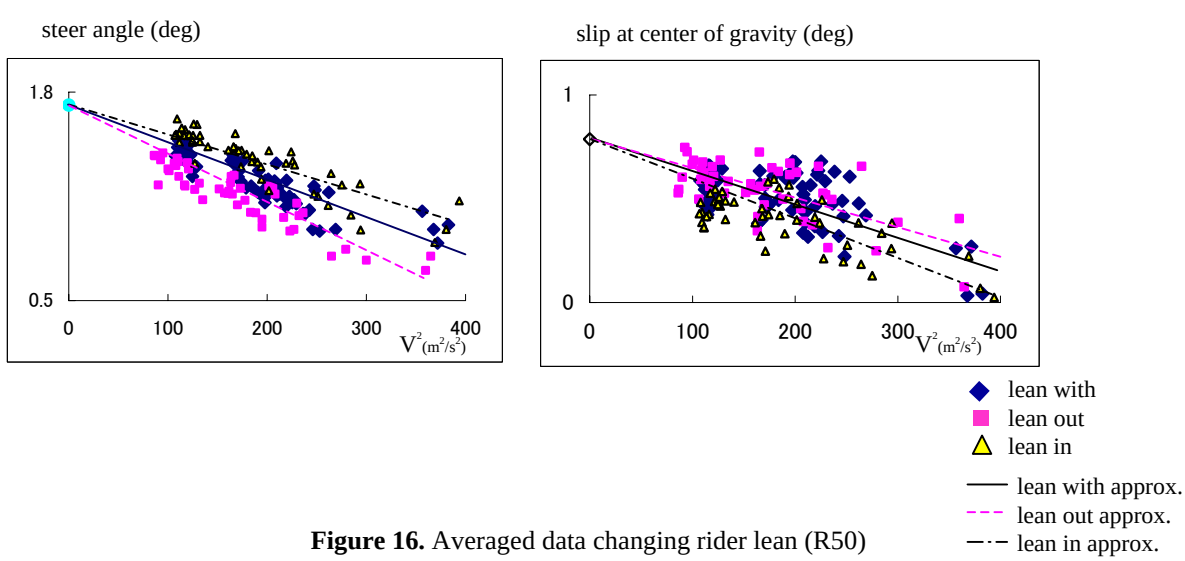

Figure 16. Averaged data changing rider lean (R50)

Next, Table 2 shows the slip angle factors obtained. The slip angle used for the slip angle factor is not the tire slip angle but the slip angle at the center of gravity of the motorcycle. The slip angle at the center of gravity was calculated similar way of the conversion the slip angle at rear tire from the optical slip sensor behind rear wheel. The optical slip sensor installed behind rear wheel determined the forward and lateral velocities directly below the sensors, corrected them for the yaw rate and the difference between the sensor position and the center of gravity position, and determined the slip angles at the center of gravity. As shown in Figs. 15 the tire slip angle at the center of gravity varied much according to the circle radius. But the tire slip angle at the center of gravity did not change much according to the lean angle. The lines in the graph for slip angle in Fig. 15 and Fig. 16 were drawn from the intercepts which meant the geometric slip angles and followed the data by the least squares method.

Lastly, when we look at the relationship between the square of the velocity and the absolute value of the hold-steering torque, the hold-steering torque differs for each circle radius. However, if we limit our analysis to the data for identical circle radii, the relationship between the square of the velocity and the hold-steering torque is nearly proportional, and it is possible to determine the slope angle for this relationship. The lines in the graph for steering torque in Fig. 15 were drawn from the origin and followed the data by the least squares method. As shown in Fig. 13, the hold-steering torque varies greatly depending on the rider's lean angle, and therefore care must be exercised when comparing results obtained from different riders.

Table 1. Stability Factor

radius/lean	geometric steering angle(deg)	stability factor (s^2/m^2)
20/with	4.30	-0.00227
30/with	2.86	-0.00180
50/with	1.72	-0.00125
50/out	1.72	-0.00177
50/in	1.72	-0.00105

Table 2. Slip Angle Factor

radius/lean	geometric slip angle(deg)	slip angle factor (s^2/m^2)
20/with	1.97	-0.00415
30/with	1.31	-0.00224
50/with	0.79	-0.00204
50/out	0.79	-0.00181
50/in	0.79	-0.00244

Table 3. Steering Torque Factor

radius/lean	steering torque factor (Ns^2/m)
20/with	0.156
30/with	0.0704
50/with	0.0302

7 CONCLUSIONS

In this study we introduced three activities that were part of our efforts to realize a quantitative development method for motorcycles. These activities included obtaining tire slip angle measurement results for a motorcycle during steady-state cornering. The three activities are summarized as follows.

First, we introduced the measurement results from our testing and research, starting with the tire slip angle of a motorcycle during steady-state cornering.

The tire slip angle measurement results obtained from the steady-state cornering test via the inertia GPS sensor were compared with the measurement results obtained at the same time via the optical slip sensor and determined to be similar. Therefore, we were able to demonstrate that it is possible to measure the tire slip angle even with the large roll angles that are unique to motorcycles. By demonstrating that it is possible to measure the tire slip angle with good accuracy, we were able to open a new path to more detailed investigations of the dynamics characteristics of motorcycles.

Furthermore, we also were able to observe that the tire slip angle continued to change in one direction as if drifting during cornering. This result demonstrated that it is possible to obtain new knowledge from measuring the tire slip angle that could not be obtained by simply estimating the tire slip angle from the other measurement results. In addition, we also described the effects of the differences in the rider's lean posture on various measurement values, starting with the tire slip angle. We found that differences in the rider's lean angle have little effect on the steering angle and Fy, but do have major effects on the hold-steering torque and tire slip angle.

Second, we verified the results that were obtained through simulation.

The measurement data that was obtained was compared to the simulation results and we showed that in many cases both results consistently corresponded with each other. Furthermore, in the case of the testing that was conducted in this research, the differences in the rider's posture, lean-in, lean-with, and lean-out, almost corresponded to the differences produced in the simulation by a 10 cm shift in the rider's weight to the right or left.

Third, we validated the evaluation indexes.

We substituted the measurement results into the steering index proposed by Kageyama et al. and determined the stability factors ,the slip angle factors, and steering torque factors.

Because stability factors and slip angle factors are not easily affected by the rider's lean posture, they have the potential of being an excellent index. However, since the steering torque factors varies greatly depending on the rider's lean posture, the testing method must be carefully considered.

By continuing to accumulate steady-state cornering test data on a wider variety of vehicles, we will be able to discuss maneuverability using index values.

Furthermore, we plan to take the next step beyond the steady-state cornering test and expand the scope of our research to include the format of tests for evaluating transient characteristics and characteristics of tire grip limit situations.

REFERENCES

[1]. Ishii,H., Tezuka,Y., "Considerations of Turning Performance for Motorcycle," SETC pp. 383-389, 1997
[2]. Kageyama, I., Kuriyagawa, Y.,"Characteristics of Steady State Turnig for Two-wheeled Vehicle - Breaking behavior using quasi-steady state analysis" JSEA No.108-08 pp. 17-20, 2008 (in Japanese)
[3]. Fujii,S., "Development of Robust Rider Controlling Model for Scooter." AVEC04, Vol. 64, No. 4 pp. 9-12, 2004
[4]. Shinagawa,A., Fujii,S.,"A Study on Three-Dimensional Course Model for Motorcycle", AVEC06 p575-580, 2006
[5]. H.B.Pacejka: "Tyre and Vehicle Dynamics", Butterworth -Heinemann, 2002
[6]. Vittore Cossalter: "MOTORCYCLE DYNAMICS (Second Edition)", 2006
[7]. RT User Manual, http://www.oxts.com/downloads/rtman.pdf
[8]. Data Sheet CORREVIT S-350, http://www.corrsys-datron.com/Support/Data_Sheets/Datasheets-Sensors/cds-d_S-350_e.pdf

ACKNOWLEDGEMENT

The authors would like to express thanks to Mr. Sven Jansen and Mr. Bart Scheepers of TNO Science and Industry / Automotive for their support to the present study.